MRS Communications

https://doi.org/10.1557/s43579-020-00003-x

MRS Communications

Prospective Article

Growing silk fibroin in advanced materials for food security

Hui Sun and **Benedetto Marelli,** Laboratory for Advanced Biopolymers, Department of Civil and Environmental Engineering, Massachusetts Institute of Technology, Cambridge, MA 02139, USA

Address all correspondence to Benedetto Marelli at **bmarelli@mit.edu**

(Received 15 September 2020; accepted 2 December 2020)

Abstract

This perspective provides an overview of the micro-/nanofabrication methods developed for structural biopolymers, highlighting recent advances in the rapid and ease construction of complex and multifunctional silk fibroin-based devices by integrating top-down manufacturing with bottom-up molecular self-assembly. Of particular interest is the development of a new nanofabrication strategy that employs templated crystallization to direct silk fibroin folding and assembly from a suspension of disordered, random coil molecules to ordered, hierarchical mesostructured materials. Such advancements in structural biopolymers fabrication provide the basis for engineering a new generation of technical materials that can be interfaced with food and plants.

Introduction

There is a compelling need to find sustainable alternatives to synthetic polymers, non-renewable semiconductors, and metal alloys—the major building materials of our daily products. For example, 36,000 tons of intentionally added microplastic particles (IAMPs) are released to the environment annually in the European Union only, given their extensive use in a wide range of products that include certain types of fertilizers, plant protection products, leave-on and rinse-off cosmetic products, household and industrial detergents, cleaning products, paints and products used in the oil and gas industry. Starting in January 2018, the European Chemicals Agency (ECHA) examined the need for an EU-wide restriction on the use of IAMPs and in January 2019 ECHA proposed a wide-ranging restriction on IAMPs in products placed on the EU market with microplastics foreseen to be completely banned by 2025.[1] Such dramatic intervention from a policymaker indicates a clear pressure on stakeholders to develop new materials that include a programmed end in their shelf-life and possess the inherent capacity to harmlessly degrade in the environment. To have an impact on our society, these materials need to meet the stringent physical, chemical, and biological requirements involved in their daily applications while also be massively abundant and cost-competitive to allow for wide utilization. In this regard, natural polymers have been shown to hold great promises as building blocks for a new generation of green and sustainable devices. This class of polymers is synthesized and modified by living organisms and provides an opportunity not only to complement/substitute synthetic polymers, but also to engineer a new generation of multifunctional materials that can bridge the biotic/abiotic interface while minimizing environmental impact during production and end of life management. Direct utilization and reengineering of natural polymers into advanced material platforms have been widely explored in a broad range of technical fields,[2–7] from biomedicine to optoelectronics, and more recently agriculture, food safety, and security. The recent use of natural polymers as technical materials to sustainably boost crop production and mitigate the environmental impact of food production and storage is of particular interest, given the need to define new technologies to make the food infrastructure more resilient.[8,9]

Agriculture and food industries have recently seen a spike in the adoption of robotics, smart sensors, big data analysis, and biotechnology to enhance farming and food processing practices to respond to the increasing demand of food while also meeting sustainability and safety concerns.[8] Presently, the need to mitigate the environmental impact of agriculture coincides with the required increase in crop productivity to feed the ever-growing population.[10] Additionally, 30–40% of the food produced globally is wasted from farm to fork, causing the loss of 25% of the worldwide consumption of freshwater and heavily impacting the environment—global food loss and waste generate annually 4.4 GtCO2 eq, or about 8% of total anthropogenic greenhouse gas (GHG) emissions. This means that the contribution of food wastage emissions to global warming is almost equivalent (87%) to global road transport emissions and that food loss is the largest generator of GHG after China and US.[10–14] Despite these challenges, the potential benefits of materials-based innovation in the Agriculture/Food industry remain underexplored. The case for the reengineering of natural polymers into advanced materials to make the food system more resilient and sustainable is then particularly compelling. Natural polymers are abundantly present on dry land and in the oceans. Among natural polymers, structural biopolymers are the major components of self-assembling and structurally hierarchical natural systems and are considered

the building blocks of life. Structural polysaccharides such as cellulose, alginate, chitosan, and agarose and their modifications are heavily used in the food and agriculture industries in various applications that leverage the encapsulation, fluid thickening, and water absorption properties of these biopolymers. Additionally, structural proteins extracted from food such as zein, casein, gelatin, whey-, egg-, and legume-derived proteins are processed in materials that positively impact food and agriculture by providing binding and mechanical support for food engineering, delivery of pesticides, and fertilizers. These applications showcase the successful use of natural polymers as materials for food and agriculture but the limited development of techniques to micro-/nanofabricate these proteins hinders their use as advanced materials that can open new opportunities at the interface with food, crops, and plants.

With this commentary, we argue that a class of structural proteins—structural exoproteins, that has been engineered by selective pressure to work outside of microorganisms in direct contact with the environment, can be engineered and fabricated in advanced materials to work in the food and agriculture industry. Structural exoproteins include silks, suckerins, keratins, and resilins and possess a high stability for a wide range of temperature (up to 200°C), pH ($2 < pH < 10$), mineral oils, organic solvents, and denaturing agents. Structural exoproteins have been recently exploited for micro-/nanofabrication enabling the engineering of high-performing, nanostructured, hierarchical, cm-scale materials that can modulate gas transport, water diffusion, heat dissipation, and micro-organism adhesion.[15–17] Of particular interest to the scientific community has been the case of silk fibroin, a highly abundant protein (2×10^8 kg/year) that the domesticated *Bombyx mori* caterpillars produce to make cocoons during the 5th instar stage of growth. Silk fibroin possesses in fact a property called polymorphism, which enables its water-based processing into water-soluble or water-insoluble end materials, depending on the molecular structure of the protein (i.e., random coil or β-sheet, respectively). In this regard, silk fibroin has been considered as a universal material for protein nanomanufacturing[18–20]; silk polymorphism provides an opportunity to modulate materials properties (molecular structure, water solubility, surface energy, thermal reflow, adhesion, self-assembly) during the development of new material fabrication strategies, which result in the design of proof-of-concepts that can then be applied to other structural biopolymers, e.g., the manufacturing of nanostructured silk fibroin materials with soft lithography and electron-beam lithography techniques has opened the door to the use of these techniques with other biopolymers.[21,22]

Using silk fibroin as an example, this commentary attempts to provide some insights on the opportunities offered by structural biopolymers as a technical material platform to enhance food safety and security. An overview of the micro-/nanofabrication methods with structural biopolymers is presented, highlighting recent advances in construction of complex and multifunctional silk fibroin-based devices by merging top-down manufacturing with bottom-up molecular self-assembly. Particular attention is given to a newly developed nanofabrication strategy that employs templated crystallization to direct silk fibroin folding and assembly from a suspension of random coil molecules to hierarchical mesostructured materials. After reviewing such advancements in biopolymer fabrication and their essential role for engineering a new generation of smart materials, we will introduce several proof-of-concepts to demonstrate how the reengineering of silk fibroin in advanced materials can underpin new biopolymer-based technologies with a positive impact on food safety and security.

Micro-/nanofabrication with silk fibroin

Native *Bombyx mori* silk fiber is composed of two silk fibroin filaments glued by sericin—a group of soluble glycoproteins.[23,24] The sericin proteins cover the surface of silk fibroin in the cocoons and generally need to be removed for biomedical applications to reduce potential inflammation in the human body[25] and for optoelectronic applications to increase the purity of silk fibroin. The regeneration of silk fibroin from *Bombyx mori* cocoons has now been a well-established process, which contains three major steps—degumming, resuspension, and dialysis (Fig. 1(a)).[26] In the degumming step, cocoons are boiled in a 0.02 M Na_2CO_3 solution to remove sericin proteins, which also massively degrades silk fibroin, with longer degumming time corresponding to more severe degradation of silk fibroin.[27,28] For example, undegraded native silk fibroin heavy chain has a monodisperse molecular weight (MW) of ~ 390 kDa, while regenerated silk fibroin shows a smear of MW distribution from undegraded chains to fragments as small as 30–40 kDa. Longer degumming time was reported to generate silk fibroin proteins of lower MW average and larger MW variance, which in turn affects the rheological properties of the silk fibroin suspension and mechanical properties of the end materials formed from these proteins.[28] The dried silk fibers obtained after the degumming step can then be suspended in deionized water using several techniques that include exposure to chaotropic ions or ionic liquids.[26,29] One of the most successful protocols used in the literature involves exposure to 9.3 M Lithium Bromide (LiBr) at 60°C for 4 h.[26] Lithium bromide is a chaotropic salt which at high concentrations is able to break the intra-/intermolecular hydrogen bonds of silk fibroin, thereby enabling dissolution of the silk fibers. Finally, the silk fibroin-LiBr suspension is dialyzed against deionized water for 2–3 days to remove the LiBr, followed by centrifugation to get rid of undissolved impurities and large aggregates, generating a purified silk fibroin-water suspension.

One way to functionalize silk fibroin is by simply dispersing various dopants in the silk fibroin suspension (Fig. 1(b)). A variety of dopants have been proved to work well with silk fibroin suspension, including but not limited to gold nanoparticles/nanorods, quantum dots, reporting dyes, antibiotics, growth factors, fluorescent proteins, enzymes, antibodies, bacteria, siRNA/DNA/plasmid, etc.[30–32] The all-water-based

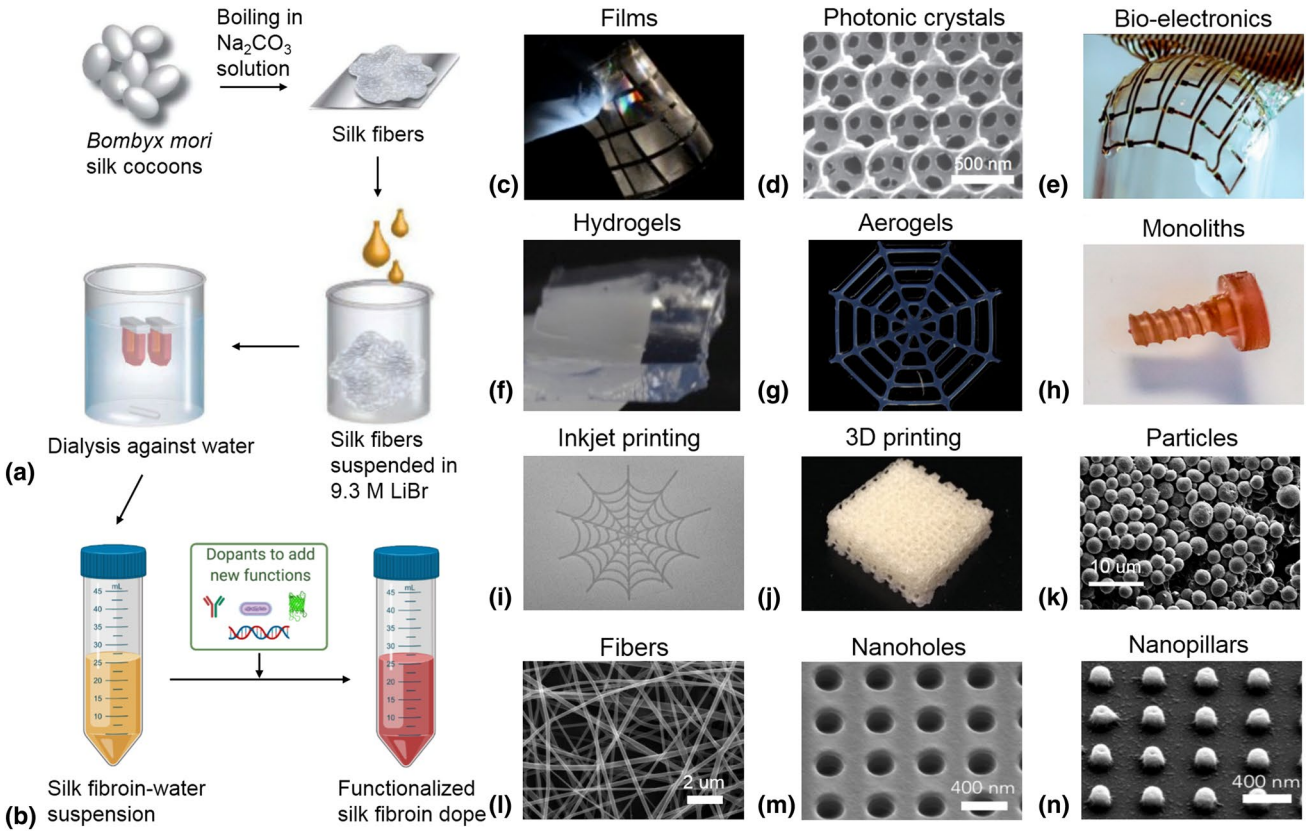

Figure 1. An overview of materials fabrication with silk fibroin. (a) Schematic of silk fibroin regeneration from *Bombyx mori* cocoons. Reproduced with permission from Ref. 26, copyright 2011, Springer Nature. (b) Functionalization of the aqueous silk fibroin suspension by adding dopants such as antibodies, microorganisms, fluorescent proteins, and siRNA/DNA/plasmid. (c)–(n) Examples of achievable forms through micro-/nanofabrication with silk fibroin: (c) Free-standing transparent films. Reproduced with permission from Ref. 35, copyright 2015, Royal Society of Chemistry. (d) 3D photonic crystals. Reproduced with permission from Ref. 38, copyright 2012, Springer Nature. (e) Bioresorbable substrates for ultrathin conformal bioelectronics. Reproduced with permission from Ref. 42, copyright 2010, Springer Nature. (f) Hydrogels. (g) Aerogels. Reproduced with permission from Ref. 52, copyright 2017, Springer Nature. (h) Machinable monoliths. Reproduced with permission from Ref. 53, copyright 2017, National Academy of Sciences. (i) 2D patterns by inkjet printing. Reproduced with permission from Ref. 31, copyright 2015, Wiley–VCH Verlag GmbH & Co. KGaA, Weinheim. (j) 3D constructs by extrusion-based bioprinting. (k) Microspheres. Reproduced with permission from Ref. 60, copyright 2014, Wiley–VCH Verlag GmbH & Co. KGaA, Weinheim. (l) Nanofibers. Reproduced with permission from Ref. 29, copyright 2004, Elsevier Inc. (m)–(n) Arrays of nanoholes (m) and nanopillars (n). Reproduced with permission from Ref. 65, copyright 2014, Springer Nature.

ambient environment of silk fibroin processing (i.e., neutral pH and room temperature) allows for incorporation of labile chemical and biological components with minimal loss of activity at the point of material fabrication, thereby enabling direct embedment of biochemical functions in the biopolymer-based end material. Silk fibroin is also known to retain the bioactivity of those incorporated labile components over extended periods of time, making it an appealing material substrate for the fabrication of sustainable and smart devices that can work at the biotic/abiotic interface.

Using silk fibroin suspension (either doped or undoped) as the starting material, a variety of constructs with different formats and dimensionalities, and of structural features spanning from nanometers to macroscale have been achieved (Fig. 1(c)–(n)). Here, we introduce some of the most representative micro-/nanofabrication methods explored with silk fibroin. By direct casting or spin coating of the silk fibroin suspension on a substrate, silk fibroin self-assembles into a thin film as water evaporates, with achievable thickness ranging from tens of nanometers to hundreds of micrometers by varying the starting silk fibroin concentration and processing conditions.[33] When casting on a relatively hydrophobic substrate, the formed silk film can be easily peeled off afterwards, resulting in a self-standing, transparent, and extremely flexible film which can be bent or folded for many times without breaking. More importantly, as silk fibroin suspension can easily infiltrate voids of the underlying substrate, by casting it on a patterned or structured substrate (e.g., hexagonally packed PMMA nanoparticle arrays), the self-assembled silk film can replicate the underlying surface topography and feature sizes down to less than 10 nm.[34] In combination with the optical transparency of the silk films, a variety of

photonic structures can be fabricated, including diffraction gratings (Fig. 1(c)),[34,35] holograms,[36] microprism and microlens arrays,[37] and photonic crystals (Fig. 1(d)).[38–40] As the degradation lifetime of silk fibroin constructs can be programmed from seconds to years by controlling the crystallinity of silk fibroin during material self-assembly and processing, silk-based optical devices can also be used as self-analyzing platforms to provide spectral and biochemical fingerprints of various incorporated components.[37,41] For example, silk fibroin microprism arrays doped with therapeutics were used as implantable and degradable drug delivery systems where the drug release profile can be optically monitored by measuring variance in the surface reflectance over time.[37] The programmable dissolution rates in water along with the mechanically flexible feature of silk fibroin thin films also make it an appropriate supporting substrate for bioresorbable, ultrathin electronics that can conform to soft and curvilinear surfaces, enabling intimate and non-invasive integration with complex biological tissues such as brains (Fig. 1(e)).[42–44] Such silk-based bioelectronics devices were fabricated through a simple transfer printing of electrode arrays directly onto drop cast silk films.

Besides thin films and lattice-based formats, hydrogels can be formed through a sol–gel transition of the silk fibroin suspension triggered by external inputs such as electric fields,[45] sonication,[46] vortexing,[47] low pH,[48] and natural aging at high concentrations over several weeks.[49] Such triggers are known to induce random coils to β-sheet transitions of silk fibroin, resulting in brittle silk gels of a whitish appearance.[50] Alternatively, silk hydrogels can be obtained via enzymatic crosslinking of silk fibroin chains (Fig. 1(f)). This is achieved through formation of covalent dityrosine bonds catalyzed by horseradish peroxidase (HRP) in the presence of hydrogen peroxide.[51] The enzymatically crosslinked silk hydrogels are optically clear, highly elastic, and possess minimal β-sheet contents, in contrast to the non-transparent gels introduced earlier which are rich in β-sheets. Formation of dityrosine bonds also imparted the silk hydrogels with significantly enhanced blue fluorescence under UV irradiation. Dehydration of the enzymatically crosslinked hydrogels in ethanol followed by critical point drying results in silk aerogels (Fig. 1(g)) that are extremely lightweight but mechanically strong (being able to sustain a load more than 4000 times its own weight).[52] From the silk gels formed by natural aging or electrogelation, further dehydration through controlled water evaporation generates silk monoliths of semicrystalline nature and partial thermoplasticity (Fig. 1(h)), allowing for machining and polishing of the monoliths into customized shapes and structures.[53]

The aqueous silk fibroin suspension also facilities its usage as functional bioinks for printing-based fabrication. With inkjet printing (Fig. 1(i)), a customized library of inkjet-printable, functional silk inks was developed by doping silk fibroin suspension with gold nanoparticles, enzymes, antibiotics, growth factors, and antibodies.[31] Rheological properties of the as-prepared silk inks can be tuned by varying the molecular weight and concentration of silk fibroin in solution, to ensure good printability of the silk inks (i.e., dimensionless number $1 < Z = (d\rho\gamma)^{1/2}/\eta < 10$, where d is the nozzle diameter, ρ, γ, and η are the density, surface tension, and viscosity of the silk inks, respectively). A variety of substrates including papers, agar plates, petri dishes, and laboratory gloves were used as supports for the printed patterns. Depending on the additives incorporated in the silk inks, multiple functional devices were demonstrated as proof-of-concepts, such as surface plasmonic resonance-based thermal imaging enabled by printing of silk-gold nanoparticles, inhibition zone of bacterial growth generated from silk-antibiotics inks, topographical control over human mesenchymal stem cells (h-MSC) differentiation through printed patterns of bone morphogenetic protein 2 (BMP-2)-doped silk, and colorimetric bacterial sensors printed with polydiacetylene/IgG antibody-silk inks. In all cases, silk fibroins are found to stabilize the incorporated components and preserve their functions and bioactivities over extended periods of time after printing of the bioinks. More recently, screen-printing of silk inks was utilized for large-scale patterning of conformal substrates such as textiles.[54] To match the shear-thinning property of inks required for screen-printing, the inks are formulated by combining a thickener (sodium alginate) and a plasticizer (glycerol) with regenerated silk fibroin. This formulation is further made reactive and responsive by addition of reporter molecules such as pH indicators and enzymes, enabling fabrication of a sensing T-shirt with printed colorimetric patterns for personalized health monitoring and performance optimization. Three-dimensional (3D) bioprinting is another commonly used method to facilely produce 3D macroscopic constructs made of biomaterials, which can potentially be used as implantable tissue engineering scaffolds or artificial organs to name a few.[55–57] In the case of 3D printing of silk constructs (Fig. 1(j)), extrusion-based direct writing is often employed, where aqueous silk fibroin inks are printed into a coagulation medium such as a methanol bath[58] or a colloidal suspension of nanoclay particles in polyethylene glycol (PEG).[59]

Finally, we introduce fabrication of silk micro-/nanostructures with feature sizes from several micrometers down to tens of nanometers. For example, silk microspheres with a decent monodispersity can be generated by using a co-flow capillary device where a continuous phase of poly(vinyl alcohol) (PVA) is flowed over a discrete phase of silk fibroin.[60,61] Breaking off the discrete silk phase in the bulk PVA stream leads to formation of silk droplets which then condense to spheres in the micron to submicron range (Fig. 1(k)). The sphere diameters can be tuned by adjusting the concentration of PVA and silk fibroin, volumetric flow rates of the two streams, and silk fibroin molecular weight (which has a direct influence on the viscosity of the silk phase). Another extensively studied form of silk is fibers or fibrous mats which can be massively produced through electrospinning (Fig. 1(l)).[29,62,63] Spinnability of a silk dope depends critically on its viscosity and surface tension. For this reason, organic solvents such as

hexafluoroisopropanol (HFIP) and formic acid (FA) are predominantly used for spinning dopes, due to their high volatility and low surface tension.[64] Protein concentrations higher than 10 wt% are generally required to ensure high viscosity. To further extend the library of achievable silk forms at the nanoscale, lithography-based nanofabrication techniques such as electron-beam lithography,[65,66] ion-beam lithography,[67] and multi-photon lithography[68,69] were employed. Here, because of its polymorphic nature, silk fibroin conformations can be regulated through interactions with an electron beam, making it capable to function as both a positive and a negative resist. To be a positive resist, spin-coated silk films are crystallized followed by electron-beam exposure on selected areas to de-crystalize silk fibroin molecules. Development with water then removes the amorphous silk fibroin, generating arrays of nanoholes (Fig. 1(m)). To work as a negative resist, spin-coated silk films are left in the amorphous state before exposure to electron beams. The electron beams used in this case are of much higher doses so that they are able to crystalize amorphous silk fibroin molecules, making it water-insoluble. The unexposed areas are then washed away by water, resulting in arrays of nanopillars (Fig. 1(n)). By changing the masks used, two-dimensional photonic crystals composed of nanoholes and nanopillars with different center-to-center spacings can be fabricated, presenting variant structural colors.[65]

Merging top-down with bottom-up

While the top-down fabrication techniques described in the previous section (i.e., printing, electrospinning, and lithography) possess great utility in manufacturing structures at a certain length scale, generation of hierarchically structured materials still remains a challenge for pure top-down methodologies. In this scenario, the study and biomimicry of natural material assembly provides an opportunity to learn universal rules about material nanomanufacturing. Natural materials are usually hierarchically organized with structural features spanning multiple length scales.[70] Prominent examples include wood, bone, tendon, nacre, silk fibers, and mussel threads, which have long been a source of inspiration for the fabrication of synthetic materials that mimic the structural organization of their natural counterparts to integrate multiple functions in a single material format. In natural systems, in fact, directed bottom-up assembly of various molecular building blocks (e.g., DNA, proteins, polysaccharides, lipids, and inorganics) constitutes the key of material generation, with superior capabilities to manipulate structures especially at the molecular and sub-nanometer scale, which can rarely be achieved with any of the currently available top-down techniques. Therefore, the strategy of combining top-down manufacturing with bottom-up self-assembly stands out and has been explored to make a variety of material formats, from DNA-mediated nanoparticle superlattices[71,72] to structural protein-based dynamic devices with stimuli-responsiveness.[73,74]

olid transition process combined with traditional lathe-based machining was exploited to fabricate 3D monoliths with multiple engineered functions embedded in a single material format.[53] The process starts with an in-depth investigation of silk fibroin conformation and morphology at different assembly stages by means of cryogenic transmission electron microscopy (cryo-TEM). Micrographs obtained by cryo-TEM depict that silk fibroin possesses nanomicellar, nanofibrillar, and bulk structures when in suspension, gel, and solid states, respectively (Fig. 2(a)). In particular, β-sheet configurations are visible in the cryo-TEM image of silk fibroin solids. The interplay between silk fibroin and water was found to be a key factor in driving silk fibroin assembly, which in turn determines the properties of the end constructs. Differential scanning calorimetry (DSC) thermograms show a decrease in free water and an increase in crystallinity and thermal stability of silk fibroin as the sol–gel-solid transition proceeds. The presence of free and bound water in silk fibroin matrix imparts partial thermoplasticity to the silk monoliths, as indicated by the occurrence of plastic deformation upon heating the silk constructs above certain temperature. For the same reason, pressure and heat can be utilized to imprint microstructures on the surface of silk solids. Due to the high crystallinity, silk solids possess enough mechanical strength to be machined and polished into various shapes (Fig. 2(b)). Designed functions are embedded by adding water-soluble dopants to the silk fibroin suspension at the point of material self-assembly. Demonstrator devices include silk fibroin-polydiacetylene (PDA) pins that undergo a blue-to-red chromatic change when stresses in the construct reach its yield point (Fig. 2(c)) and a silk fibroin screw doped with gold nanorods which can be heated on demand in response to infrared light (Fig. 2(d)).

Besides dehydration-driven self-assembly, conformational transitions of silk fibroin can also be regulated by exposure to water vapor (WV), methanol vapor (MV), and ultraviolet (UV) irradiation. Silk polymorphism controlled by such external stimuli in conjunction with top-down surface patterning is then employed to create dynamic and responsive wrinkling systems where on-demand tuning of surface morphologies and physical properties can be achieved.[74] Briefly, wrinkled surfaces are produced by heating and subsequent cooling of a silk/PDMS bilayer (Fig. 2(e)). The wrinkles can be partially erased by selective exposure to WV, MV, or UV light using shadow masks to generate patterned wrinkles, or completely eliminated by flood exposure. During this process, molecular rearrangement of silk fibroin chains triggered by WV, MV, and UV stimuli induces gradual release of the compressive stress within the bilayer composite, leading to relaxation or erasure of the wrinkled topography. Wrinkle formation and erasure dynamics can be monitored by measuring light transmittance through the system, which depends critically on the initial silk fibroin conformations (Fig. 2(f)). Multiple functional devices were demonstrated based on the stimuli-responsive nature of silk wrinkles. For example, patterned silk wrinkles are fabricated by selective exposure to UV irradiation, where exposed

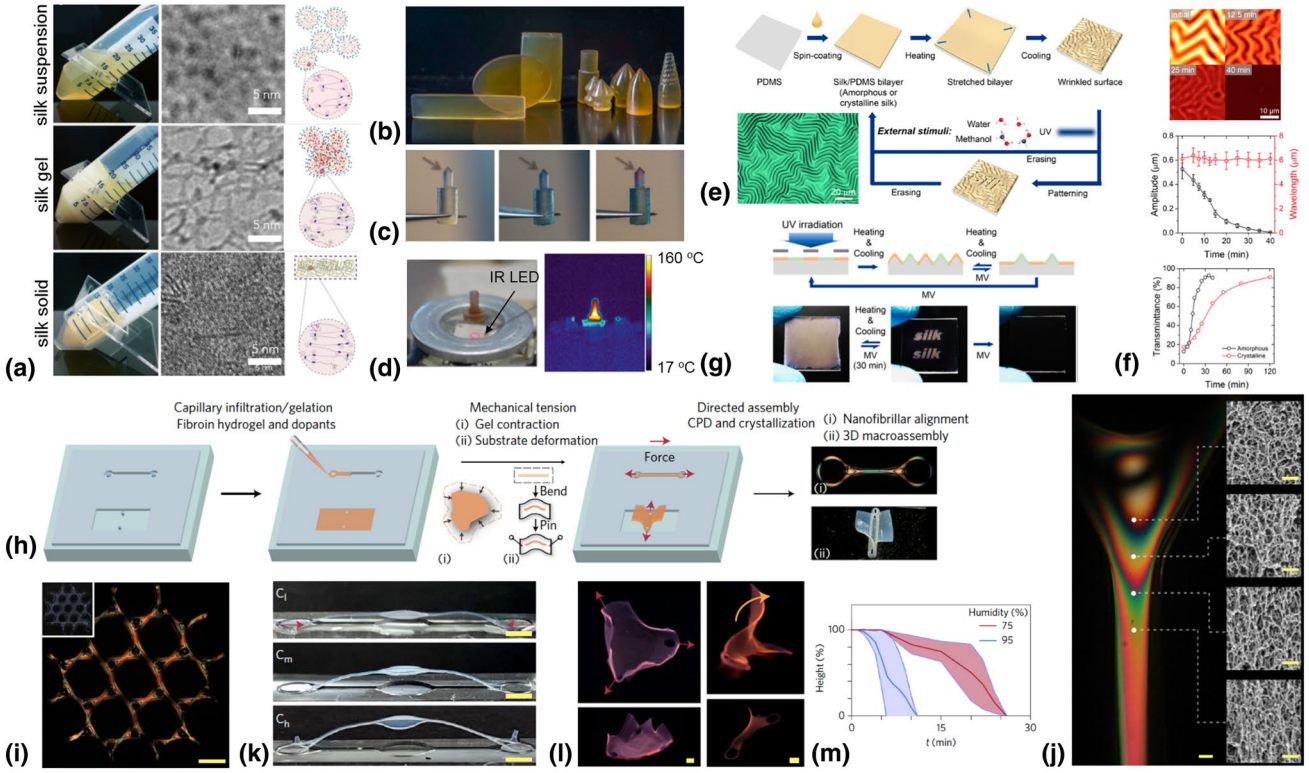

Figure 2. Merging top-down nanofabrication with bottom-up self-assembly. (a) Macroscopic and nanoscopic investigation of silk fibroin self-assembly and relative schematics of the proposed mechanism. Cryo-TEM images obtained at different stages of silk fibroin self-assembly depict a nanomicellar, nanofibrillar, and bulk structure for silk fibroin when in suspension, gel, and solid forms, respectively. β-sheet configurations are visible in the micrograph of silk solid. (b) Representative three-dimensional silk constructs fabricated by machining of the silk monoliths. (c) Mechanical failure visualized through colorimetric responses of PDA vesicles embedded in the silk fibroin matrix. (d) A silk fibroin screw doped with gold nanorods can be heated up to 160°C under illumination of a LED that emits infrared light (850 nm). (a)–(d). Reproduced with permission from Ref. 53, copyright 2017, National Academy of Sciences. (e) Schematic of the process for preparing reversible wrinkled patterns. Silk fibroin solution is spin-coated on a soft PDMS substrate to form a silk/PDMS bilayer composite. Surface wrinkling is induced by heating and subsequent cooling of the silk/PDMS bilayer. The wrinkles can be partially erased by selective exposure to WV, MV, or UV light using shadow masks to generate patterned wrinkles, or completely eliminated by flood exposure. An optical microscopy image captured with a green filter depicts a typical wrinkled surface. (f) Wrinkle evolution induced by exposure to MV: AFM images showing the erasure process of amorphous silk wrinkles (top); corresponding time dependence of wrinkle amplitude A and wavelength λ (middle); transmittance change of the wrinkled surfaces over time (bottom). (g) Schematic for the preparation of an MV-revealable pattern (top row). Wrinkles formed from UV-treated silk fibroin possess different de-wrinkling dynamics when exposed to MV, enabling reversible read and permanent erasure of the UV-written pattern. (e)–(g) Reproduced with permission from Ref. 74, copyright 2019, National Academy of Sciences. (h) Schematic of the mechanically directed silk fibroin assembly into nanofibrillar networks. Aqueous silk fibroin mixed with HRP and H_2O_2 is first infiltrated and gelled in a predesigned PDMS mold. Mechanical tension is then introduced by either contraction of the silk gel in mixtures of ethanol and water or direct deformation of the PDMS substrate. Critical point drying is then applied to generate the final silk aerogel composed of a nanofibrillar network. (i) Representative silk aerogels (inset) showing remarkable birefringence under polarized light. Scale bar, 1 mm. (j) Optical birefringence and the associated internal nanofibrillar morphology revealed by SEM. Increasing stress and birefringence correspond to increasing nanofibrillar alignment and orientation. Scale bars, 200 μm (optical) and 400 nm (SEM). (k) Buckling of high-aspect-ratio beams under contraction. C_l, C_m, and C_h indicate samples with low (10–25%), medium (25–40%), and high (>40%) contraction, respectively. Scale bars, 2 mm. (l) Reshaping thin plates into 3D folded structures by placing anchor points at the edges or around the corners. Scale bars, 2 mm. (m) Height evolution of a moisture-actuated pop-up structure over time. (h)–(m) Reproduced with permission from Ref. 52, copyright 2017, Springer Nature.

areas are rendered to possess different de-wrinkling dynamics because of the UV-induced protein degradation. Exposure to MV for a short period of time allows for revealing of the UV-written pattern, due to flattening of the unexposed silk wrinkles only (Fig. 2(g)). This reversible reading process can withstand multiple cycles and the pattern can also be permanently erased by prolonged exposure to MV which allows for de-wrinkling of the UV-exposed areas, resetting the surface to its initial flat state which can again be processed by UV irradiation.

Another example deals with nanofabrication of macroscopic silk aerogels composed of aligned nanofibrillar networks at the microscale (Fig. 2(h)).[52] The nanofabrication process starts with gelation of silk fibroin suspension by reacting with HRP and hydrogen peroxide in predesigned PDMS molds of various geometries (anchors, periodic polygon lattices, and webs).

Mechanical tension is then exerted on the silk hydrogels through gel contraction in aqueous ethanol or mold deformation. Finally, the silk hydrogels under tensile stresses are critical-point-dried to generate aerogels of the same macroscopic architecture as the PDMS molds. At the microscopic level, the fabricated silk aerogels are composed of highly aligned nanofibrils, as verified by the remarkable birefringence observed under polarized light (Fig. 2(i)). Scanning electron microscopy (SEM) characterization reveals that increasing stress and optical birefringence correspond to increasing nanofibril alignment and orientation (Fig. 2(j)). This approach is then extended to fabricate three-dimensional constructs with engineered nanofibrillar hierarchy that possess environmental responsiveness. For example, a linear construct comprised of a circular disk in the middle supported by two slender beams at the ends is fabricated to exploit pop-up buckling induced by swelling of the silk aerogel at a certain humidity (Fig. 2(k)). Higher contractions associated with increasing birefringence (i.e., nanofibrils alignment) correlate positively with the beam buckling and pop-up height. Similarly, buckling instability is explored by placing the anchor points at the edge of thin plates or oriented around the corners to obtain controllably folded structures (Fig. 2(l)). Such constructs are also found to be moisture-responsive (Fig. 2(m)), as silk can be plasticized by water, indicating the possibility of environmentally actuating such geometries.

Templated crystallization: a paradigm shift

While more and more top-down manufacturing methods are being applied in silk fibroin-based materials to extend the scope of structural formats and complexity that can be achieved, we find that there is much less progress in the aspect of directing silk fibroin assembly from the bottom-up. All of the nanofabrication strategies introduced so far rely on silk fibroin assembly triggered by certain external input, with the most extensively used ones being water removal,[53] solvent exchange (e.g., with ethanol),[52] pH, ionic strength, temperature,[49] shear stress,[75] mechanical constraints,[52] electric field,[45] and sonication.[46] These inputs are effective in transforming silk fibroin conformation from random coils to β-sheet (i.e., disorder to order transition), but they generally do not exert further control over the folding and assembly pathway of silk fibroin and thereby do not have much influence on the resultant silk polymorphs. A question that remains largely unexplored but of critical importance is, can we nanofabricate silk fibroin into hierarchically structured materials of predefined molecular structures and mechanical properties by directing the folding and assembly of silk fibroin to follow a route that is different from its normal self-assembly pathway under those commonly used triggers? To answer this question, a technique named templated crystallization was developed, which refers to the use of organic templates (specifically, ordered peptide assemblies) to drive a phase transformation of silk fibroin from unordered to ordered conformations (Fig. 3(a)), thereby enabling further assembly of the reconfigured silk fibroin chains into higher order structures (e.g., β-sheeted nanofibrils).[76] Schematically, templated crystallization of silk fibroin works as follows:

It starts with the choice of a peptide that (1) forms ordered supramolecular assemblies, (2) binds to silk fibroin molecules, typically through the formation of hydrogen bonds or hydrophobic interactions, and (3) shares similar isoelectric point and pH stability with silk fibroin. In this parameter space, the highly repetitive $(GAGAGS)_n$ sequence of the hydrophobic domains of silk fibroin heavy chain provides an opportunity to use peptides 'homologous' to silk fibroin as template materials. A dodecapeptide of sequence GAGSGAGAGSGA[77] (noted as $(GAGSGA)_2$ thereafter for brevity) was chosen due to its ability to self-assemble into regular nanowhisker-like supramolecular oligomers of dimensions around $200 \times 20 \times 4$ nm (Fig. 3(a), i–iii). Structural characterization of the nanowhiskers indicates a highly ordered β-sheet conformation (Fig. 3(a), iv). Silk fibroin regenerated from *Bombyx mori* cocoons, on the contrary, possesses a random coil dominant conformation (Fig. 3(a), v). Because of its hydrophobic-hydrophilic multiblock copolymer primary structure (Fig. 3(a), viii), above a critical micelle concentration (c.m.c.), silk fibroin self-assembles into micelles to minimize hydrophobic interactions with water (Fig. 3(a), vi and viii–ix).[24,53] It is hypothesized that exposure to highly ordered β-sheet nanowhiskers results in disassembly of silk fibroin micelles, enabling the formation of a transition state at a higher energy, where their hydrophobic domains are exposed to water before folding into a highly ordered (i.e., lower energy) β-sheet structure (Fig. 3(a), ix–xi). Assembly of the folded silk fibroin chains on the nanowhisker surfaces then results in thicker and longer $(GAGSGA)_2$-silk nanocomplexes that are stabilized mainly by hydrophobic interactions (Fig. 3(a), xii). TEM imaging along with structural characterization by circular dichroism (CD) spectroscopy confirmed the hypothesis on which templated crystallization is based, by showing that silk fibroin molecules assemble on the nanowhisker seeds and form thicker and longer nanocomplexes in the beginning, followed by growth of thinner nanofibrils branching out from the nanocomplexes (Fig. 3(b)). This process is associated with a continuous increase in the β-sheet content of silk fibroin as indicated by the CD spectra (Fig. 3(c)).

An important merit of templated crystallization is its ability to engineer silk polymorphs by varying the peptide seeds used. To this end, a coiled-coil peptide from honeybee silk[78,79] (noted as HBSP thereafter for brevity)—ALKAQSEEEAASARANAATAATQSALEG was chosen, which self-assembles into supramolecular oligomers of a non-trivial alpha-helical component and much lower beta-sheet contents (Figs. 3d, e), as compared to the dodecapeptide $(GAGSGA)_2$ (Fig. 3(a), iv). When mixed with silk fibroin, it drives a similar disorder to order transition of silk fibroin and nanofibrils assembly (Fig. 3(f)), but the beta-content and intermolecular arrangements of silk fibroin seeded by the two peptides are clearly different, as shown by the X-ray scattering spectra which depict different d-spacings of silk fibroin that result from the templates' effects (Fig. 3(g)).

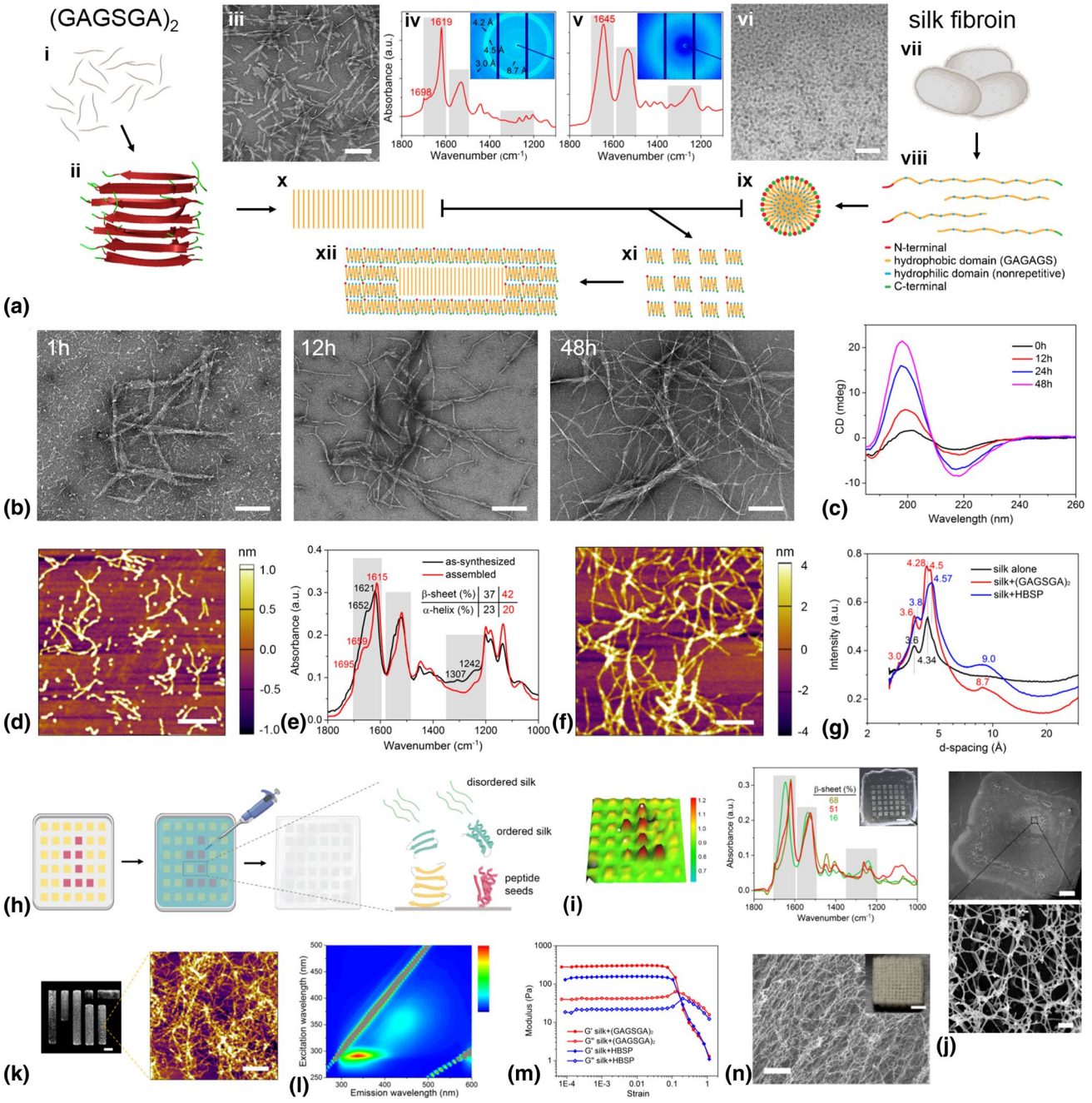

It is further demonstrated that templated crystallization as a bottom-up molecular assembly process can be easily combined with various top-down manufacturing techniques to generate macroscopic hierarchical materials with complex shapes and programmable functions. In particular, two different strategies are pursued. The first example deals with an epitaxial-like growth process (Fig. 3(h)), which starts by depositing two different peptide seeds on a substrate to form a predesigned pattern. The peptide-coated substrate is then exposed to silk fibroin solution to allow for disorder to order transition of silk fibroin at the peptide-coated area. At the end of templated crystallization, the solution dries out, from which a free-standing silk film is generated. We can clearly see the background checkerboard pattern due to the transparency change of silk film associated with crystallization of silk fibroin (Fig. 3(i), inset); however, the intentionally embedded number "1" in the pattern is not identifiable by visual inspection. Nonetheless, it becomes evident with ATR-FTIR mapping of the patterned silk film (Fig. 3(i)), as the infrared spectroscopy is able to identify subtle differences in molecular structures of silk fibroin seeded by different peptides, so that the patterned free-standing silk film serves as an information storage/encryption device.

◂**Figure 3.** Templated crystallization of silk fibroin. (a) Schematic of the templated crystallization process: A dodecapeptide $(GAGSGA)_2$ self-assembles into nanowhisker-like supramolecular oligomers of a highly ordered β-sheet structure (i–iv), which are used as seeds to drive a phase transformation of silk fibroin (vii, viii) from unordered (v, vi) to ordered conformations (ix–xi), thereby enabling further assembly of the silk fibroin chains into β-sheeted nanofibrils (xii). (b) Negative-stain TEM images of silk nanofibrils seeded by $(GAGSGA)_2$ nanowhiskers at 1 h, 12 h, and 48 h, depicting a directed assembly of silk fibroin on the $(GAGSGA)_2$ nanowhiskers. Scale bars, 200 nm. (c) CD spectra of silk fibroin seeded by $(GAGSGA)_2$ nanowhiskers, showing an increase in the β-sheet content of silk fibroin over time. (d) Atomic force micrograph of HBSP self-assembled in water, showing nanoassemblies of irregular shapes and dimensions. Scale bar, 400 nm. (e) ATR-FTIR spectra of HBSP powders as synthesized and upon assembly from an aqueous suspension, indicating a combination of β-sheet (main peaks at 1621 and 1615 cm^{-1}) and α-helix (shoulders at 1652 and 1659 cm^{-1}) conformations. (f) Atomic force micrograph of silk nanofibrils seeded by HBSP nanoassemblies. Scale bar, 400 nm. (g) 1D WAXS spectra of naturally aged silk fibroin, $(GAGSGA)_2$- and HBSP-templated silk fibroin, depicting different molecular packing (i.e., d-spacings) of silk fibroin, due to the templates' effects. (h) Schematic of the process for epitaxial-like growth of silk fibroin on substrates modified with peptide seeds. Yellow and red denote $(GAGSGA)_2$ and HBSP seeds, respectively. (i) ATR-FTIR map of a patterned silk film (inset in the right panel, scale bar, 3 mm) fabricated by the process shown in (h) revealing the hidden Arabic numeral "1" which is indiscernible by visual or microscopic inspection. Representative spectra at the three asterisks in the FTIR map are given in the right panel. (j) SEM characterization of a surface functionalized with mesoporous and nanofibrillar silk fibroin that grows on the pre-deposited seeds. Scale bars, 200 μm (top) and 300 nm (bottom). (k) Inkjet printing of a silk nanofibrils suspension obtained through templated crystallization. Scale bars, 1 mm (left) and 1 μm (right). (l) Fluorescence excitation-emission matrix (EEM) of suspensions of silk nanofibrils seeded by $(GAGSGA)_2$. (m) Evaluation of the rheological properties of silk nanofibrils gels—measurements of storage and loss moduli (G' and G'', respectively). (n) Continuous printing of the silk nanofibrils gel into a three-dimensional construct (inset) and a representative SEM image of the internal structure. Scale bars, 5 mm (inset) and 200 nm (SEM). (a), (h) Adapted with permission from Ref. 76, copyright 2020, Springer Nature. (b)–(g), (i)–(n) Reproduced with permission from Ref. 76, copyright 2020, Springer Nature.

Alternatively, the same strategy can be used to functionalize a surface with mesoporous and nanofibrillar silk fibroin through templated crystallization on pre-immobilized seeds (Fig. 3(j)). Another demonstration is development of silk nanofibril-based printable inks. In this regard, silk nanofibrils suspension is coupled with inkjet printing to pattern surfaces with nanofibrillar mats (Fig. 3(k)). A gel-like ink is developed by concentrating the silk nanofibril suspension for extrusion-based 3D printing. Such inks are composed of densely packed nanofibrillar networks, as characterized by the fluorescence excitation-emission matrix (EEM, Fig. 3(l)), where the excitation and emission maxima at 355 and 438 nm, respectively (i.e., fluorescence in the visible range) indicate the presence of hydrogen bond-rich protein fibrils.[80] Rheological measurements of the nanofibrillar gels show that they possess good elasticity required for extrusion-based 3D printing (Fig. 3(m)). SEM characterization of the printed materials confirms the deposition of nanofibrillar silk fibroin (Fig. 3(n)), where the nanofibrils could also be aligned by controlling the nozzle dimension and printing speed.

Templated crystallization of silk fibroin, in our view, is a directed assembly process that is fundamentally different from previously reported bottom-up nanofabrication strategies, which are based on self-assembly of silk fibroin upon exposure to external fields and generally have little control over the molecular folding and assembly pathway. The ability to topographically regulate growth of silk nanofibrils into macroscopic materials also represents an advancement when compared to the formation of silk nanofibrillar networks directed by mechanical constraints,[52] exfoliation of silk fibers into nanofibrils,[81,82] or electrospinning,[64] as it allows control over silk polymorphs and the associated nanomechanical properties, which is essential for engineering the next-generation functional materials with programmed properties and biological responses.

Applications in food and agri-tech industry

Beyond the broad range of technical fields that silk fibroin has found applications in, an emerging and growing interest is being placed on applying silk fibroin-based materials and devices to solve some of the most pressing issues in agriculture, food safety, and security.[83–85] The world population is projected to reach 9.7 billion by 2050, which requires an estimation of 70% increase in food production to feed the growing population.[86] Additionally, there are 800 million people currently living in food insecurity, yet at the same time we have tons of food wasted every second from around the world.[87] Reduction of food waste thus plays a pivotal role in mitigating the food crisis we are facing by improving food security and reducing loss of economic values. One significant portion of food waste comes from premature deterioration of perishable crops. In this scenario, formation of edible coatings that wrap around such crops as a protection barrier against fast exchange of water and oxygen as well as microbial contamination serves as a useful means to decelerate spoilage of perishable food and extend its shelf-life postharvest.[83,88] As a biopolymer that has been designated as a Generally Regarded as Safe (GRAS) food item by the US Food and Drug Administration, silk fibroin represents a good candidate for use as edible food coatings. This is particularly true considering that silk fibroin can easily form conformal thin films that are transparent, tasteless and odorless, mechanically robust and flexible, biodegradable, and that possess low permeability to oxygen and water vapors due to the abundance of hydrophobic groups in the silk fibroin primary structure—all are compelling properties for an edible coating material. Indeed, it was shown that silk fibroin coatings can preserve the freshness and firmness of perishable fruits such as strawberries and bananas for longer periods of time by effectively slowing fruit respiration and restricting dehydration (Fig. 4(a), (b)).[83] Coating of such fruits with silk fibroin is achieved through a two-phase process. Firstly, fruits are dip-coated in 1 wt%

silk fibroin suspension repeatedly up to 4 times. Then the silk fibroin-coated fruits are treated with water vapor under low vacuum (i.e., the water annealing post-processing) for different periods of time to modulate the β-sheet contents in silk fibroin. It was found that silk fibroin coatings of higher β-sheet contents possess much lower oxygen permeability, further slowing down fruit respiration rate as measured by CO_2 production and show statistically significant improvement in maintaining fruit freshness and firmness over the studied storage time (Fig. 4(a), (b)).

Alternatively, the mechanical and gas barrier properties of food coatings can be regulated by formulation of polymer blends that leverage the distinct properties of each components and achieve synergistic effects contributed from all constituents involved. For example, silk fibroin is blended with poly(vinyl alcohol) (PVOH) at different ratios for use as food coating and packaging materials.[89] The choice of PVOH is based on its GRAS status, low water vapor and oxygen permeability, immiscibility with silk fibroin, good thermal and chemical stability, and high stretchability. Of all the SF:PVOH ratios studied, SF:PVOH 1:1 results to be the most promising material candidate for edible food coatings as demonstrated by efficacy tests on preservation of fresh-cut apples (Fig. 4(c), (d)). Over the course of storage post cut, apple slices coated with SF:PVOH 1:1 show statistically significant lower weight loss as compared to uncoated controls and slices coated with pure silk fibroin and PVOH (Fig. 4(c)). SF:PVOH 1:1 films also present a better preservation of the apple slices from browning/oxidation as compared to pure silk fibroin and PVOH films (Fig. 4(d)). The remarkable property of SF:PVOH 1:1 coatings is arguably due to its bi-layered structure that results from a phase separation of silk fibroin and PVOH during simultaneous self-assembly, where silk fibroin forms a layer that is in intimate contact with the apple flesh and PVOH forms an outer protective barrier.

While efforts to reduce food waste are important for enhancing food security, a significant increase in crop productivity is still required to feed the ever-growing population. Seed enhancement technologies are therefore of critical importance by enabling germination of seeds in degraded lands, reducing use of agrochemicals and boosting crop yields. Particularly, the development of advanced seed coatings has emerged as a promising route to control seed surface properties, locally enrich soil with nutrients and positively affect seed water uptake.[90] In this regard, a prominent example showcases the use of silk fibroin-trehalose blends as seed coating materials

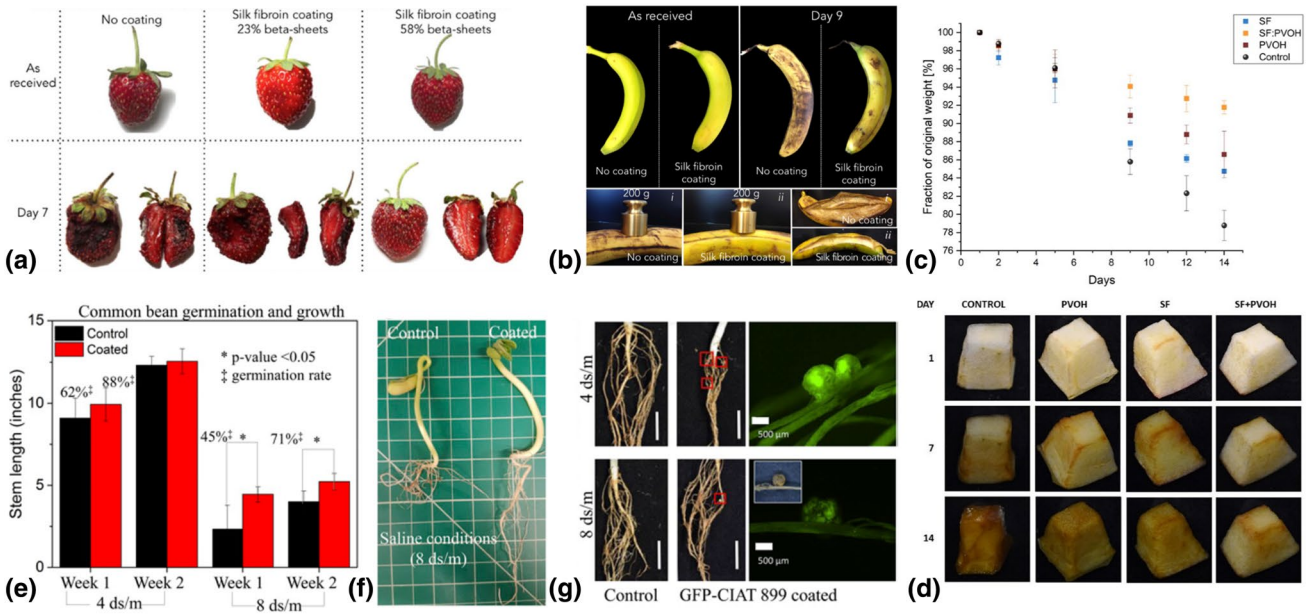

Figure 4. Silk fibroin-based edible coatings for perishable food preservation and seed germination boost in saline soil. (a) Time-lapse images of strawberry ripening. Strawberries coated with silk fibroin of higher β-sheet contents exhibit the best quality at day 7. (b) Time-lapse images of banana ripening showing that silk fibroin coatings decrease the ripening rate (top panel). Silk fibroin-coated bananas have better firmness and fresher flesh at day 9, when compared to uncoated controls (bottom panel). (a), (b) Reproduced with permission from Ref. 83, copyright 2016, Springer Nature. (c) Weight loss of apple slices coated with different materials and uncoated controls. (d) Time-lapse images of apple slices coated with different materials and uncoated controls. SF:PVOH 1:1 coatings present the best preservation of the apple slices from browning/oxidation. (c), (d) Reproduced with permission from Ref. 89, copyright 2020, American Chemical Society. (e) Germination rate and stem growth of coated and uncoated *Phaseolus vulgaris* seeds over a 2-week period in non-saline (4 ds/m) and saline (8 ds/m) soils. (f) Comparison of the root systems of coated and uncoated seeds. (g) Root colonization by the rhizobacteria as indicated by formation of nodules. Scale bar, 1 cm. (e)–(g) Reproduced with permission from Ref. 84, copyright 2019, National Academy of Sciences.

that encapsulate, preserve, and deliver biofertilizers upon sowing to boost seed germination and mitigate soil salinity (Fig. 4(e)–(g)).[84] The biofertilizer used here is made of plant growth promoting rhizobacteria (PGPRs) that are able to fix nitrogen and increase availability of nutrients for plant roots.[91] Such biomaterial formulation for seed coatings synergistically employs the film-forming, payload encapsulation, preservation, and tunable biodegradation capabilities of silk fibroin and the ability of trehalose to support survival of rhizobacteria during desiccation and resuscitation. Statistically significant improvement in both germination rate and seedling growth of coated *Phaseolus vulgaris* seeds is observed, as compared to uncoated controls (Fig. 4(e)). Interestingly, the effects of seed coatings in boosting germination and seedling growth are more evident for seeds grown in saline soil. Coated seeds grow into seedlings that are taller and possess longer and more articulated roots in comparison to uncoated controls (Fig. 4(f)). Nodule formation assessed by visual inspection and fluorescence microscopy confirms root colonization by the rhizobacteria (Fig. 4(g)).

Other demonstrations of silk fibroin-based devices that are of particular interest in agriculture include microneedle patches for precision payload delivery *in planta* (Fig. 5(a)–(c)).[85] For this application, silk fibroin blended with silk fibroin-derived hydrophilic peptides (Cs) is fabricated into a microneedle-like device, dubbed "phytoinjector", which is capable of targeting various plant tissues for deployment of several payloads. Using tissue-specific phytoinjectors, custom payloads (from small molecules to large proteins) can be delivered into tomato plants vasculature to study material transport in xylem and phloem (Fig. 5(a)). Additionally, independent delivery of luciferin and luciferase in the vasculature results in a bioluminescence reaction in the tissues downstream the injection site (Fig. 5(b)). In tobacco, *Agrobacterium*-loaded phytoinjectors can achieve gene transfer to and expression in shoot apical meristem and in leaves at various stages of growth (Fig. 5(c)). Further tuning of material composition (i.e., silk:Cs ratio) yields another device, dubbed "phytosampler", which is capable of sampling plant sap for detection of metabolites.

By extending the idea of using silk microneedle patches to sample fluids from plant, it was found that such device also possesses great utility as pathogen sensors for food quality monitoring (Fig. 5(d)–(f)).[92] Here, the silk microneedle patches are water annealed for 8 h post fabrication to induce formation of pores larger than a few microns inside the silk needles. Bioinks

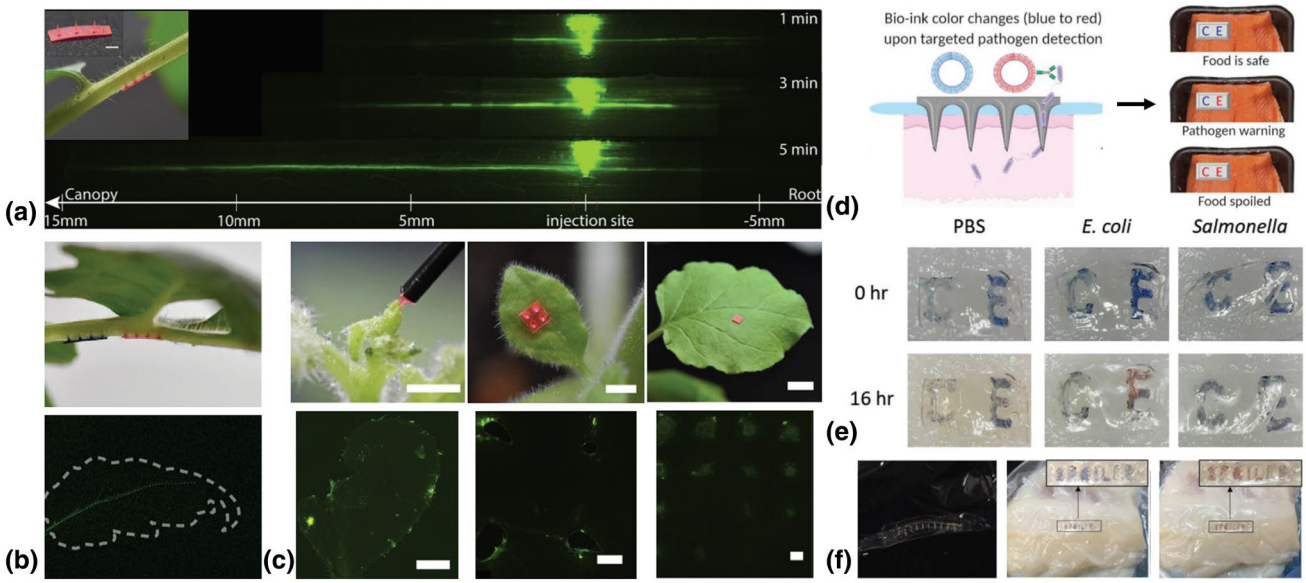

Figure 5. Silk microneedle patches as phytoinjectors for precision payload delivery *in planta* and as foodborne pathogen sensors. (a) A tomato plant injected in the petiole by a phytoinjector loaded with rhodamine 6G (inset, scale bar: 1 mm), and fluorescent images showing 5(6)-carboxyfluorescein diacetate delivered to and transported in xylem, from roots to canopy, 1, 3, and 5 min post injection. (b) Two phytoinjectors loaded with different payloads (luciferin for blue injectors and luciferase for red ones) targeting petiole's xylem concurrently (top panel). By providing external ATP and Mg^{2+}, the leaf vein emits light (exposure time 120 s, bottom panel). (c) *Agrobacterium*-mediated gene transfer to shoot apical meristem (left), a young leaf (middle), and a mature leaf (right). Expression of green fluorescent protein (GFP) is observed in leaf cells by fluorescence microscopy (bottom panel). Scale bars: 2 mm (top) and 500 μm (bottom). (a)–(c) Reproduced with permission from Ref. 85, copyright 2020, Wiley–VCH Verlag GmbH & Co. KGaA, Weinheim. (d) Schematic illustration of using silk microneedle patches to sample fluids from food which then triggers a colorimetric response of the printed PDA patterns upon detection of pathogens. (e) Application of silk microneedle patches with PDA patterns printed on top to fish fillets contaminated with foodborne bacteria. A color change of the printed patterns from blue to red can be identified within 16 h post injection. (f) A silk microneedle patch penetrating a commercial food wrap (left) to detect spoilage of a packaged fish fillet. Images collected at time 0 (middle) and 4 h (right) after applying the microneedle patch. (d)–(f) Reproduced with permission from Ref. 92, copyright 2020, Wiley–VCH Verlag GmbH & Co. KGaA, Weinheim.

composed of polydiacetylene (PDA) liposomes conjugated with bacteria-specific antibodies are then printed onto the backside of the microneedle patch. Application of such microneedle sensors to packaged food (e.g., fish fillets) enables sampling and transport of fluids deep in the food tissues to the backside of the microneedle patch, where colorimetric responses of the printed PDA inks will be triggered upon detection of targeted pathogen in the food fluid (Fig. 5(d)). To verify the efficacy of such pathogen sensors, fish fillets contaminated with *Escherichia coli* and *Salmonella Typhimurium* were tested, and a color change of the printed patterns from blue to red can be identified within 16 h of microneedle application (Fig. 5(e)). Moreover, the silk microneedle patches are strong enough to penetrate not only fish flesh but also its packaging films (Fig. 5(f)), obviating the need for opening the package and sacrificing food samples required by other food inspection methods.

Conclusions and future perspectives

The ability to engineer structural biopolymers into advanced materials has been shown to benefit a broad range of technical fields, from biomedicine to optoelectronics. In this domain, silk fibroin regenerated from *Bombyx mori* cocoons is among the most-widely employed base materials for the fabrication of various high-tech and multifunctional devices, due to the material's massive abundance in nature, ease of processing, and good compatibility with a variety of abiotic and biotic components. Yet regenerated silk proteins also have some intrinsic limitations, one of which being its highly polydispersed nature in both the molecular weight and primary structure. Such polydispersity makes controlled bottom-up assembly of regenerated silk fibroin more challenging, as compared to monodispersed proteins/peptides with well-defined amino acid sequences. For example, in the case of templated crystallization of silk fibroin, monodispersed native silk fibroin extracted from the gland of *Bombyx mori* silkworms at the 5th instar show much higher nucleation and growth rates, with the formed nanofibrils having more uniform morphology and nanomechanical property.[76] Besides, when used as templates for biomineralization of inorganics such as calcium carbonate, silk fibroin of narrower molecular weight distribution was found to be more effective in generating calcium carbonate crystals with well-regulated shape and polymorph.[93] Genetic engineering/Synthetic biology then comes in as a powerful tool to construct monodispersed silk proteins with precisely defined sequences through protein expression in heterologous hosts such as *E. coli*, yeasts, and mammalian cells. This technique has gained a lot of success in production of recombinant spider silk proteins,[94,95] but for proteins of sequences similar to *Bombyx mori* silk fibroin, significant obstacles still remain, due to the difficulty in engineering recombinant DNA that encodes highly repetitive amino acid sequence. Industrialization of this process is very promisingly moving forward yet still at its infancy, due to the challenges in protein yields and costs for large-scale protein production, among others.

On the other hand, almost all protein engineering to date have involved the modification of naturally occurring ones. This is because evolution has explored only a tiny portion of the sequence space that is accessible to proteins, and although natural proteins possess remarkable efficiency in performing various functions, they may not represent the best candidate to play a certain role.[96] Likewise, engineered silk fibroin may outperform the natural protein in certain applications, e.g., coatings to preserve perishable food, as optimization of its amino acid sequence and even rational design of a new structural protein may work out to constitute a better material with lower gas permeability to further extend the food preservation time. With the development of multiple advanced computational algorithms and the emerging use of machine learning in protein design,[96–98] such efforts have become more and more important in revolutionizing the field of materials science.

Finally, we believe that templated crystallization represents a paradigm shift in nanofabrication of structural biopolymers as it allows to precisely regulate protein disorder to order transition by using templates, and achieve directed molecular assembly into higher order structures with control over polymorphism and nanomechanical properties. These features will bring new opportunities in engineering the next generation of smart materials that can be interfaced with food and plants. The ability to grow structural biopolymers into hierarchical materials with well-regulated nanostructures may enable preservation matrices of better barrier properties, delivery systems with multi-payload encapsulation and plant sensors of higher specificity and sensitivity, paving the way for transforming agriculture to be more efficient, resilient and sustainable.[99,100]

Acknowledgments

This work was supported by the Office of Naval Research (Award No. N000141812258) and the National Science Foundation (Award No. CMMI-1752172).

Compliance with ethical standards

Conflict of interest

BM is co-founder of a company, Mori Inc., that uses silk fibroin-based materials as edible food coatings to increase the shelf-life of perishable food. The use of silk fibroin as an edible coating, seed coating, and to fabricate microneedles for drug delivery in plants is protected by multiple IP positions where BM is listed as a co-inventor.

References

1. ECHA: Restricting the Use of Intentionally Added Microplastic Particles to Consumer or Professional Use Products of Any Kind—Annex XV Restriction Report (2019).
2. J.G. Rouse, M.E. Van Dyke, A review of keratin-based biomaterials for biomedical applications. *Materials* **3**, 999 (2010)

3. H. Tao, D.L. Kaplan, F.G. Omenetto, Silk materials—a road to sustainable high technology. *Adv. Mater.* **24**, 2824 (2012)
4. D.W. Ding, P.A. Guerette, J. Fu, L.H. Zhang, S.A. Irvine, A. Miserez, From soft self-healing gels to stiff films in suckerin-based materials through modulation of crosslink density and beta-sheet content. *Adv. Mater.* **27**, 3953 (2015)
5. L.Q. Li, A. Mahara, Z.X. Tong, E.A. Levenson, C.L. McGann, X.Q. Jia, T. Yamaoka, K.L. Kiick, Recombinant resilin-based bioelastomers for regenerative medicine applications. *Adv. Healthc. Mater.* **5**, 266 (2016)
6. R.M. Parker, G. Guidetti, C.A. Williams, T.H. Zhao, A. Narkevicius, S. Vignolini, B. Frka-Petesic, The self-assembly of cellulose nanocrystals: hierarchical design of visual appearance. *Adv. Mater.* **30**, 1704477 (2018)
7. S. Lee, E.S. Sani, A.R. Spencer, Y. Guan, A.S. Weiss, N. Annabi, Human-recombinant-elastin-based bioinks for 3D bioprinting of vascularized soft tissues. *Adv. Mater.* **32**, 2003915 (2020)
8. United Nations: The Role of Science, Technology and Innovation in Ensuring Food Security by 2030 (2017).
9. D. Laborde, W. Martin, J. Swinnen, R. Vos, COVID-19 risks to global food security. *Science* **369**, 500 (2020)
10. C. Mbow, C. Rosenzweig, L.G. Barioni, T.G. Benton, M. Herrero, M. Krishnapillai, E. Liwenga, P. Pradhan, M.G. Rivera-Ferre, T. Sapkota, F.N. Tubiello, Y. Xu, Food Security. in *Climate Change and Land: an IPCC Special Report on Climate Change, Desertification, Land Degradation, Sustainable Land Management, Food Security, and Greenhouse Gas Fluxes in Terrestrial Ecosystems* (2019).
11. FAO: Water for Sustainable Food and Agriculture—A Report Produced for the G20 Presidency of Germany (2017).
12. FAO and ITPS: Status of the World's Soil Resources—Main Report (2015).
13. U.S. Environmental Protection Agency: Inventory of U.S. Greenhouse Gas Emissions and Sinks (EPA 430-R-16–002, 2016, Washington).
14. C.A. Schlosser, K. Strzepek, X. Gao, C. Fant, É. Blanc, S. Paltsev, H. Jacoby, J. Reilly, A. Gueneau, The future of global water stress: an integrated assessment. *Earth's Future* **2**, 341–361 (2014)
15. L. Cera, G.M. Gonzalez, Q.H. Liu, S. Choi, C.O. Chantre, J. Lee, R. Gabardi, M.C. Choi, K. Shin, K.K. Parker, A bioinspired and hierarchically structured shape-memory material. *Nat. Mater.* (2020). https://doi.org/10.1038/s41563-020-0789-2
16. L.Q. Li, Z.X. Tong, X.Q. Jia, K.L. Kiick, Resilin-like polypeptide hydrogels engineered for versatile biological function. *Soft Matter* **9**, 665 (2013)
17. K. Deepankumar, C. Lim, I. Polte, B. Zappone, C. Labate, M.P. De Santo, H. Mohanram, A. Palaniappan, D.S. Hwang, A. Miserez, Supramolecular beta-sheet suckerin-based underwater adhesives. *Adv. Funct. Mater.* **30**, 1907534 (2020)
18. F.G. Omenetto, D.L. Kaplan, New opportunities for an ancient material. *Science* **329**, 528 (2010)
19. X. Hu, P. Cebe, A.S. Weiss, F. Omenetto, D.L. Kaplan, Protein-based composite materials. *Mater. Today* **15**, 208 (2012)
20. Z.T. Zhou, S.Q. Zhang, Y.T. Cao, B. Marelli, X.X. Xia, T.H. Tao, Engineering the future of silk materials through advanced manufacturing. *Adv. Mater.* **30**, 1706983 (2018)
21. D.W. Ding, J. Pan, S.H. Lim, S. Amini, L.F. Kang, A. Miserez, Squid suckerin microneedle arrays for tunable drug release. *J. Mater. Chem. B* **5**, 8467 (2017)
22. E. Bat, J. Lee, U.Y. Lau, H.D. Maynard, Trehalose glycopolymer resists allow direct writing of protein patterns by electron-beam lithography. *Nat. Commun.* **6**, 1–8 (2015)
23. Z.Z. Shao, F. Vollrath, Materials: surprising strength of silkworm silk. *Nature* **418**, 741 (2002)
24. H.J. Jin, D.L. Kaplan, Mechanism of silk processing in insects and spiders. *Nature* **424**, 1057 (2003)
25. G.H. Altman, F. Diaz, C. Jakuba, T. Calabro, R.L. Horan, J.S. Chen, H. Lu, J. Richmond, D.L. Kaplan, Silk-based biomaterials. *Biomaterials* **24**, 401 (2003)
26. D.N. Rockwood, R.C. Preda, T. Yucel, X.Q. Wang, M.L. Lovett, D.L. Kaplan, Materials fabrication from Bombyx mori silk fibroin. *Nat. Protoc.* **6**, 1612 (2011)
27. E.M. Pritchard, X. Hu, V. Finley, C.K. Kuo, D.L. Kaplan, Effect of silk protein processing on drug delivery from silk films. *Macromol. Biosci.* **13**, 311 (2013)
28. B.P. Partlow, A.P. Tabatabai, G.G. Leisk, P. Cebe, D.L. Blair, D.L. Kaplan, Silk fibroin degradation related to rheological and mechanical properties. *Macromol. Biosci.* **16**, 666 (2016)
29. B.M. Min, G. Lee, S.H. Kim, Y.S. Nam, T.S. Lee, W.H. Park, Electrospinning of silk fibroin nanofibers and its effect on the adhesion and spreading of normal human keratinocytes and fibroblasts in vitro. *Biomaterials* **25**, 1289 (2004)
30. S.Z. Lu, X.Q. Wang, Q. Lu, X. Hu, N. Uppal, F.G. Omenetto, D.L. Kaplan, Stabilization of enzymes in silk films. *Biomacromolecules* **10**, 1032 (2009)
31. H. Tao, B. Marelli, M.M. Yang, B. An, M.S. Onses, J.A. Rogers, D.L. Kaplan, F.G. Omenetto, Inkjet printing of regenerated silk fibroin: from printable forms to printable functions. *Adv. Mater.* **27**, 4273 (2015)
32. Y.W. Liu, Z.Z. Zheng, H. Gong, M. Liu, S.Z. Guo, G. Li, X.Q. Wang, D.L. Kaplan, DNA preservation in silk. *Biomater. Sci.* **5**, 1279 (2017)
33. B.D. Lawrence, M. Cronin-Golomb, I. Georgakoudi, D.L. Kaplan, F.G. Omenetto, Bioactive silk protein biomaterial systems for optical devices. *Biomacromolecules* **9**, 1214 (2008)
34. F.G. Omenetto, D.L. KapLan, A new route for silk. *Nat. Photonics* **2**, 641 (2008)
35. B. Marelli, F.G. Omenetto, Cashmere-derived keratin for device manufacturing on the micro- and nanoscale. *J. Mater. Chem. C* **3**, 2783 (2015)
36. M. Cronin-Golomb, A.R. Murphy, J.P. Mondia, D.L. Kaplan, F.G. Omenetto, Optically induced birefringence and holography in silk. *J. Polym. Sci. Pol. Phys.* **50**, 257 (2012)
37. H. Tao, J.M. Kainerstorfer, S.M. Siebert, E.M. Pritchard, A. Sassaroli, B.J.B. Panilaitis, M.A. Brenckle, J.J. Amsden, J. Levitt, S. Fantini, D.L. Kaplan, F.G. Omenetto, Implantable, multifunctional, bioresorbable optics. *Proc. Natl. Acad. Sci. USA* **109**, 19584 (2012)
38. S. Kim, A.N. Mitropoulos, J.D. Spitzberg, H. Tao, D.L. Kaplan, F.G. Omenetto, Silk inverse opals. *Nat. Photonics* **6**, 817 (2012)
39. Y. Wang, D. Aurelio, W.Y. Li, P. Tseng, Z.Z. Zheng, M. Li, D.L. Kaplan, M. Liscidini, F.G. Omenetto, Modulation of multiscale 3D lattices through conformational control: painting silk inverse opals with water and light. *Adv. Mater.* **29**, 1702769 (2017)
40. Y. Wang, W.Y. Li, M. Li, S.W. Zhao, F. De Ferrari, M. Liscidini, F.G. Omenetto, Biomaterial-based "structured opals" with programmable combination of diffractive optical elements and photonic bandgap effects. *Adv. Mater.* **31**, 1805312 (2019)
41. P. Domachuk, H. Perry, J.J. Amsden, D.L. Kaplan, F.G. Omenetto, Bioactive "self-sensing" optical systems. *Appl. Phys. Lett.* **95**, 253702 (2009)
42. D.H. Kim, J. Viventi, J.J. Amsden, J.L. Xiao, L. Vigeland, Y.S. Kim, J.A. Blanco, B. Panilaitis, E.S. Frechette, D. Contreras, D.L. Kaplan, F.G. Omenetto, Y.G. Huang, K.C. Hwang, M.R. Zakin, B. Litt, J.A. Rogers, Dissolvable films of silk fibroin for ultrathin conformal bio-integrated electronics. *Nat. Mater.* **9**, 511 (2010)
43. S.W. Hwang, X. Huang, J.H. Seo, J.K. Song, S. Kim, S. Hage-Ali, H.J. Chung, H. Tao, F.G. Omenetto, Z.Q. Ma, J.A. Rogers, Materials for bioresorbable radio frequency electronics. *Adv. Mater.* **25**, 3526 (2013)
44. H. Tao, S.W. Hwang, B. Marelli, B. An, J.E. Moreau, M.M. Yang, M.A. Brenckle, S. Kim, D.L. Kaplan, J.A. Rogers, F.G. Omenetto, Silk-based resorbable electronic devices for remotely controlled therapy and in vivo infection abatement. *Proc. Natl. Acad. Sci. USA* **111**, 17385 (2014)
45. G.G. Leisk, T.J. Lo, T. Yucel, Q. Lu, D.L. Kaplan, Electrogelation for protein adhesives. *Adv. Mater.* **22**, 711 (2010)
46. X.Q. Wang, J.A. Kluge, G.G. Leisk, D.L. Kaplan, Sonication-induced gelation of silk fibroin for cell encapsulation. *Biomaterials* **29**, 1054 (2008)
47. T. Yucel, P. Cebe, D.L. Kaplan, Vortex-induced injectable silk fibroin hydrogels. *Biophys. J.* **97**, 2044 (2009)
48. A.E. Terry, D.P. Knight, D. Porter, F. Vollrath, PH induced changes in the rheology of silk fibroin solution from the middle division of Bombyx mori silkworm. *Biomacromolecules* **5**, 768 (2004)
49. U.J. Kim, J.Y. Park, C.M. Li, H.J. Jin, R. Valluzzi, D.L. Kaplan, Structure and properties of silk hydrogels. *Biomacromolecules* **5**, 786 (2004)

50. A. Matsumoto, J. Chen, A.L. Collette, U.J. Kim, G.H. Altman, P. Cebe, D.L. Kaplan, Mechanisms of silk fibroin sol-gel transitions. *J. Phys. Chem. B* **110**, 21630 (2006)
51. B.P. Partlow, C.W. Hanna, J. Rnjak-Kovacina, J.E. Moreau, M.B. Applegate, K.A. Burke, B. Marelli, A.N. Mitropoulos, F.G. Omenetto, D.L. Kaplan, Highly tunable elastomeric silk biomaterials. *Adv. Funct. Mater.* **24**, 4615 (2014)
52. P. Tseng, B. Napier, S.W. Zhao, A.N. Mitropoulos, M.B. Applegate, B. Marelli, D.L. Kaplan, F.G. Omenetto, Directed assembly of bio-inspired hierarchical materials with controlled nanofibrillar architectures. *Nat. Nanotechnol.* **12**, 474 (2017)
53. B. Marelli, N. Patel, T. Duggan, G. Perotto, E. Shirman, C.M. Li, D.L. Kaplan, F.G. Omenetto, Programming function into mechanical forms by directed assembly of silk bulk materials. *Proc. Natl. Acad. Sci. USA* **114**, 451 (2017)
54. G. Matzeu, L. Mogas-Soldevila, W.Y. Li, A. Naidu, T.H. Turner, R. Gu, P.R. Blumeris, P. Song, D.G. Pascal, G. Guidetti, M. Li, F.G. Omenetto, Large-scale patterning of reactive surfaces for wearable and environmentally deployable sensors. *Adv. Mater.* **32**, 2001258 (2020)
55. K. Schacht, T. Jungst, M. Schweinlin, A. Ewald, J. Groll, T. Scheibel, Biofabrication of cell-loaded 3D spider silk constructs. *Angew. Chem. Int. Ed.* **54**, 2816 (2015)
56. R.R. Jose, M.J. Rodriguez, T.A. Dixon, F. Omenetto, D.L. Kaplan, Evolution of bioinks and additive manufacturing technologies for 3d bioprinting. *ACS Biomater. Sci. Eng.* **2**, 1662 (2016)
57. A. Lee, A.R. Hudson, D.J. Shiwarski, J.W. Tashman, T.J. Hinton, S. Yerneni, J.M. Bliley, P.G. Campbell, A.W. Feinberg, 3D bioprinting of collagen to rebuild components of the human heart. *Science* **365**, 482 (2019)
58. S. Ghosh, S.T. Parker, X.Y. Wang, D.L. Kaplan, J.A. Lewis, Direct-write assembly of microperiodic silk fibroin scaffolds for tissue engineering applications. *Adv. Funct. Mater.* **18**, 1883 (2008)
59. M.J. Rodriguez, T.A. Dixon, E. Cohen, W.W. Huang, F.G. Omenetto, D.L. Kaplan, 3D freeform printing of silk fibroin. *Acta Biomater.* **71**, 379 (2018)
60. A.N. Mitropoulos, G. Perotto, S. Kim, B. Marelli, D.L. Kaplan, F.G. Omenetto, Synthesis of silk fibroin micro-and submicron spheres using a co-flow capillary device. *Adv. Mater.* **26**, 1105 (2014)
61. U. Shimanovich, F.S. Ruggeri, E. De Genst, J. Adamcik, T.P. Barros, D. Porter, T. Muller, R. Mezzenga, C.M. Dobson, F. Vollrath, C. Holland, T.P.J. Knowles, Silk micrococoons for protein stabilisation and molecular encapsulation. *Nat. Commun.* **8**, 1–9 (2017)
62. X.H. Zhang, M.R. Reagan, D.L. Kaplan, Electrospun silk biomaterial scaffolds for regenerative medicine. *Adv. Drug Deliv. Rev.* **61**, 988 (2009)
63. C.R. Wittmer, T. Claudepierre, M. Reber, P. Wiedemann, J.A. Garlick, D. Kaplan, C. Egles, Multifunctionalized electrospun silk fibers promote axon regeneration in the central nervous system. *Adv. Funct. Mater.* **21**, 4232 (2011)
64. M. Humenik, G. Lang, T. Scheibel, Silk nanofibril self-assembly versus electrospinning. *Wires Nanomed. Nanobi* **10**, e1509 (2018)
65. S. Kim, B. Marelli, M.A. Brenckle, A.N. Mitropoulos, E.S. Gil, K. Tsioris, H. Tao, D.L. Kaplan, F.G. Omenetto, All-water-based electron-beam lithography using silk as a resist. *Nat. Nanotechnol.* **9**, 306 (2014)
66. N. Qin, S.Q. Zhang, J.J. Jiang, S. Gilbert Corder, Z.G. Qian, Z.T. Zhou, W. Lee, K.Y. Liu, X.H. Wang, X.X. Li, Z.F. Shi, Y. Mao, H.A. Bechtel, M.C. Martin, X.X. Xia, B. Marelli, D.L. Kaplan, F.G. Omenetto, M.K. Liu, T.H. Tao, Nanoscale probing of electron-regulated structural transitions in silk proteins by near-field IR imaging and nano-spectroscopy. *Nat. Commun.* **7**, 1–8 (2016)
67. J.J. Jiang, S.Q. Zhang, Z.G. Qian, N. Qin, W.W. Song, L. Sun, Z.T. Zhou, Z.F. Shi, L. Chen, X.X. Li, Y. Mao, D.L. Kaplan, S.N.G. Corder, X.Z. Chen, M.K. Liu, F.G. Omenetto, X.X. Xia, T.H. Tao, Protein bricks: 2D and 3D bio-nanostructures with shape and function on demand. *Adv. Mater.* **30**, 1705919 (2018)
68. Y.L. Sun, Q. Li, S.M. Sun, J.C. Huang, B.Y. Zheng, Q.D. Chen, Z.Z. Shao, H.B. Sun, Aqueous multiphoton lithography with multifunctional silk-centred bio-resists. *Nat. Commun.* **6**, 8612 (2015)
69. M.B. Dickerson, P.B. Dennis, V.P. Tondiglia, L.J. Nadeau, K.M. Singh, L.F. Drummy, B.P. Partlow, D.P. Brown, F.G. Omenetto, D.L. Kaplan, R.R. Naik, 3D printing of regenerated silk fibroin and antibody-containing microstructures via multiphoton lithography. *ACS Biomater. Sci. Eng.* **3**, 2064 (2017)
70. J.W.C. Dunlop, P. Fratzl, Biological composites. *Annu. Rev. Mater. Res.* **40**, 1 (2010)
71. M.X. Wang, S.E. Seo, P.A. Gabrys, D. Fleischman, B. Lee, Y. Kim, H.A. Atwater, R.J. Macfarlane, C.A. Mirkin, Epitaxy: programmable atom equivalents versus atoms. *ACS Nano* **11**, 180 (2017)
72. Q.Y. Lin, E. Palacios, W.J. Zhou, Z.Y. Li, J.A. Mason, Z.Z. Liu, H.X. Lin, P.C. Chen, V.P. Dravid, K. Aydin, C.A. Mirkin, DNA-mediated size-selective nanoparticle assembly for multiplexed surface encoding. *Nano Lett.* **18**, 2645 (2018)
73. M. Li, Y. Wang, A.P. Chen, A. Naidu, B.S. Napier, W.Y. Li, C.L. Rodriguez, S.A. Crooker, F.G. Omenetto, Flexible magnetic composites for light-controlled actuation and interfaces. *Proc. Natl. Acad. Sci. USA* **115**, 8119 (2018)
74. Y. Wang, B.J. Kim, B. Peng, W.Y. Li, Y.Q. Wang, M. Li, F.G. Omenetto, Controlling silk fibroin conformation for dynamic, responsive, multifunctional, micropatterned surfaces. *Proc. Natl. Acad. Sci. USA* **116**, 21361 (2019)
75. C. Holland, J.S. Urbach, D.L. Blair, Direct visualization of shear dependent silk fibrillogenesis. *Soft Matter* **8**, 2590 (2012)
76. H. Sun, B. Marelli, Polypeptide templating for designer hierarchical materials. *Nat. Commun.* **11**, 1–13 (2020)
77. R.W. Hao, J.M. Zhang, T. Xu, L. Huang, J.R. Yao, X. Chen, Z.Z. Shao, Characterization and assembly investigation of a dodecapeptide hydrolyzed from the crystalline domain of Bombyx mori silk fibroin. *Polym. Chem.* **4**, 3005 (2013)
78. T.D. Sutherland, S. Weisman, H.E. Trueman, A. Sriskantha, J.W.H. Trueman, V.S. Haritos, Conservation of essential design features in coiled coil silks. *Mol. Biol. Evol.* **24**, 2424 (2007)
79. T.D. Sutherland, J.S. Church, X.A. Hu, M.G. Huson, D.L. Kaplan, S. Weisman, Single honeybee silk protein mimics properties of multi-protein silk. *PLoS ONE* **6**, e16489 (2011)
80. D. Pinotsi, L. Grisanti, P. Mahou, R. Gebauer, C.F. Kaminski, A. Hassanali, G.S.K. Schierle, Proton transfer and structure-specific fluorescence in hydrogen bond-rich protein structures. *J. Am. Chem. Soc.* **138**, 3046 (2016)
81. F. Zhang, Q. Lu, J.F. Ming, H. Dou, Z. Liu, B.Q. Zuo, M.D. Qin, F. Li, D.L. Kaplan, X.G. Zhang, Silk dissolution and regeneration at the nanofibril scale. *J. Mater. Chem. B* **2**, 3879 (2014)
82. S.J. Ling, C.M. Li, K. Jin, D.L. Kaplan, M.J. Buehler, Liquid exfoliated natural silk nanofibrils: applications in optical and electrical devices. *Adv. Mater.* **28**, 7783 (2016)
83. B. Marelli, M.A. Brenckle, D.L. Kaplan, F.G. Omenetto, Silk fibroin as edible coating for perishable food preservation. *Sci. Rep.* **6**, 25263 (2016)
84. A.T. Zvinavashe, E. Lim, H. Sun, B. Marelli, A bioinspired approach to engineer seed microenvironment to boost germination and mitigate soil salinity. *Proc. Natl. Acad. Sci. USA* **116**, 25555 (2019)
85. Y.T. Cao, E. Lim, M.L. Xu, J.K. Weng, B. Marelli, Precision delivery of multiscale payloads to tissue-specific targets in plants. *Adv. Sci.* **7**, 1903551 (2020)
86. FAO, IFAD, UNICEF, WFP, WHO: The State of Food Security and Nutrition in the World 2019: Safeguarding Against Economic Slowdowns and Downturns (2019)
87. FAO: Global Food Losses and Food Waste—Extent, Causes and Prevention (2011)
88. V. Falguera, J.P. Quintero, A. Jimenez, J.A. Munoz, A. Ibarz, Edible films and coatings: structures, active functions and trends in their use. *Trends Food Sci. Technol.* **22**, 292 (2011)
89. E. Ruggeri, D.Y. Kim, Y.T. Cao, S. Fare, L. De Nardo, B. Marelli, A multi-layered edible coating to extend produce shelf life. *ACS Sustain. Chem. Eng.* **8**, 14312 (2020)
90. S. Pedrini, D.J. Merritt, J. Stevens, K. Dixon, Seed coating: science or marketing spin? *Trends Plant Sci.* **22**, 106 (2017)
91. B. Lugtenberg, F. Kamilova, Plant-growth-promoting rhizobacteria. *Annu. Rev. Microbiol.* **63**, 541 (2009)

92. D. Kim, Y.T. Cao, D. Mariappan, M.S. Bono, A.J. Har, B. Marelli, A microneedle technology for sampling and sensing bacteria in the food supply chain. *Adv. Funct. Mater.* (2020)
93. C. Cheng, Z.Z. Shao, F. Vollrath, Silk fibroin-regulated crystallization of calcium carbonate. *Adv. Funct. Mater.* **18**, 2172 (2008)
94. X.X. Xia, Z.G. Qian, C.S. Ki, Y.H. Park, D.L. Kaplan, S.Y. Lee, Native-sized recombinant spider silk protein produced in metabolically engineered *Escherichia coli* results in a strong fiber. *Proc. Natl. Acad. Sci. USA* **107**, 14059 (2010)
95. H. Chung, T.Y. Kim, S.Y. Lee, Recent advances in production of recombinant spider silk proteins. *Curr. Opin. Biotechnol.* **23**, 957 (2012)
96. P.S. Huang, S.E. Boyken, D. Baker, The coming of age of de novo protein design. *Nature* **537**, 320 (2016)
97. A.R. Thomson, C.W. Wood, A.J. Burton, G.J. Bartlett, R.B. Sessions, R.L. Brady, D.N. Woolfson, Computational design of water-soluble alpha-helical barrels. *Science* **346**, 485 (2014)
98. Z. Qin, L.F. Wu, H. Sun, S.Y. Huo, T.F. Ma, E. Lim, P.Y. Chen, B. Marelli, M.J. Buehler, Artificial intelligence method to design and fold alpha -helical structural proteins from the primary amino acid sequence. *Extreme Mech. Lett.* **36**, 100652 (2020)
99. J.P. Giraldo, H.H. Wu, G.M. Newkirk, S. Kruss, Nanobiotechnology approaches for engineering smart plant sensors. *Nat. Nanotechnol.* **14**, 541 (2019)
100. G.V. Lowry, A. Avellan, L.M. Gilbertson, Opportunities and challenges for nanotechnology in the agri-tech revolution. *Nat. Nanotechnol.* **14**, 517 (2019)